AIP Publishing

This manuscript was accepted by Appl. Phys. Lett. Click here to see the version of record.

Metastable defect response in CZTSSe from admittance spectroscopy

Mark J. Koeper[1], Charles J. Hages[2], Jian V. Li,[3] Dean Levi,[4] Rakesh Agrawal[1,*]

[1]School of Chemical Engineering, 480 Stadium Mall Drive, Purdue University, West Lafayette, IN, 47907 USA

[2]Department of Structure and Dynamics of Energy Materials, Helmholtz-Zentrum für Materialien und Energie (HZB), Hahn-Meitner Platz 1,D-14109, Berlin, Germany

[3]RFM3214, Department of Physics, Texas State University, San Marcos, TX 78666, USA

[4]National Renewable Energy Laboratory, 15013 Denver W Pkwy, Golden, CO, USA

*corresponding author: agrawalr@purdue.edu

Abstract

Admittance spectroscopy is a useful tool used to study defects in semiconductor materials. However metastable defect responses in non-ideal semiconductors can greatly impact the measurement and therefore the interpretation of results. Here, admittance spectroscopy was performed on $Cu_2ZnSn(S,Se)_4$ (CZTSSe) where metastable defect response is illustrated due to the trapping of injected carriers into a deep defect state. To investigate the metastable response, admittance measurements were performed under electrically and optically relaxed conditions in comparison to a device following a low level carrier-injection pretreatment. The relaxed measurement demonstrates a single capacitance signature while two capacitance signatures are observed for the device measured following carrier-injection. The deeper level signature, typically reported for kesterites, is activated by charge trapping following carrier injection. Both signatures are attributed to bulk level defects. The significant metastable response observed on kesterites due to charge trapping obscures accurate interpretation of defect levels from admittance spectroscopy and indicates great care must be taken when performing and interpreting this measurement on non-ideal devices.

$Cu_2ZnSn(S,Se)_4$ (CZTSSe) has been the focus of extensive research as a potential absorber layer for photovoltaic applications due to its direct band gap, high absorption coefficient, and because it is comprised of earth abundant elements.[1,2] Admittance spectroscopy (AS) has been used to study CZTSSe by several research groups[3–6] as this technique is useful to quantify defect activation energies and distributions as well as the dielectric constant of the depleted semiconductor[7]. Typically one or two capacitance signatures are observed in admittance spectroscopy of kesterites, with a range of activation energies (E_A) reported by various research groups.[3–6,8] Such variations in the reported capacitance signatures have been linked with variations in absorber processing conditions, compositional variations, and alkali content in the absorber layer. However, an additional influence on the capacitance response can originate from metastable defect behavior, which has been demonstrated in the similar $Cu(In,Ga)(S,Se)_2$ (CIGSSe)[9,10] material system. The impact of metastabilities on the analysis of AS has not been shown for the kesterite material system, despite the observed influence this behavior has on other optoelectronic measurements such as current-voltage (JV) measurements[11,12] and quantum efficiency (QE) measurements[13]. In particular, charge-trapping into defect states – recently observed for kesterites[14,15] – can have a significant impact on AS measurements; since AS utilizes a small voltage perturbation with no current injection, metastable responses can be activated upon carrier

ACCEPTED MANUSCRIPT

15 September 2024 04:34:55

AIP Publishing

This manuscript was accepted by Appl. Phys. Lett. Click here to see the version of record.

injection under various measurement conditions. Therefore the experimental conditions require careful consideration.

In this work, we demonstrate the large impact metastability in CZTSSe has on AS measurements before and after metastable changes are induced. We find metastable defect response occurs due to charge trapping following the injection of carriers into a relaxed device. Therefore, the interpretation of capacitance signatures in admittance spectroscopy of kesterites can be significantly affected by the measurement conditions. Specifically, capacitance signatures are dependent upon the voltage and illumination history of the device. Here, a relaxed CZTSSe sample exhibits a single capacitance signature while two capacitance signatures are observed on the device following low-level carrier injection. Following carrier injection, both capacitance signatures have higher activation energies than that of the relaxed measurement. Voltage dependent AS indicates the capacitance signatures are due to bulk defects in the kesterite absorber.

CZTSSe solar cells discussed here-in were fabricated by the selenization of CZTS nanoparticles on a Mo substrate, as described by Misken et al.[16] Devices were completed with the structure CdS (50 nm)/ZnO (80 nm)/ITO (220 nm)/Ni-Al grids. The device used in this study demonstrates 8.1% total area power conversion efficiency under AM1.5 illumination conditions at 1 sun; light and dark IV curves are shown in Fig. S1 of the supporting information (SI). AS measurements were performed with an Agilent 4294A impedance analyzer. All capacitance is calculated assuming a parallel circuit model shown in Fig. S2 of the SI.[7] All measurements were performed using a 15 mV_{rms} AC signal with frequencies ranging from 100 Hz to 1 MHz and completed in the dark. The measurements were completed starting at low temperatures (c. 60-80 K) and increasing to room temperature (c. 300 K). The relaxed sample was allowed to equilibrate in the dark at the lowest temperature for 2 hours with no voltage or current source. Metastable defect response was activated by a carrier-injection pretreatment (CIP) which consists of sourcing the sample with 1 mA/cm^2 forward bias current for 5 minutes prior to each frequency sweep measurement; the CIP treatment was repeated at each fixed temperature and fixed DC voltage bias. Similar behavior is observed following carrier injection from illumination of the device. Note the device can take as long as 2 hours to fully relax at cryogenic temperatures following carrier-injection. The relaxation process is monitored by comparing Nyquist (i.e. reactance vs. resistance) plots over time until changes are no longer observed. For the voltage dependent AS experiment, the cell was subjected to a DC voltage bias ranging from -1.0 to +0.2 V_{DC} with a 0.1 V_{DC} step size.

Capacitance as a function of frequency and temperature is shown in Fig. 1 for the CZTSSe sample under relaxed conditions and following CIP to activate metastable defect response; a large variation in the sample response between the two measurement conditions is observed. The relaxed sample exhibits a single capacitance signature (D1) of c. 12-15 nF/cm^2 followed by a rise in the capacitance with increasing temperature. This rise in the capacitance signal following the D1 response is attributed to contributions from deep defects. Comparing this with the measurement after the CIP, there is a similar capacitance signature of c. 12-15 nF/cm^2 (D1) but an additional capacitance signature of c. 30 nF/cm^2 (D2). For the device following the CIP, there is also a rise in capacitance at higher temperatures following the D1 and D2 response, indicating deeper defects play a similar role in both conditions. At low temperature and high frequency both measurements converge to c. 8.5 nF/cm^2, which we interpret as the geometric capacitance (C_G) of the absorber layer. This results in a dielectric value of approximately 8.5ε_0 (where ε_0 is the permittivity of free space), similarly reported by our group[8] and several others[3,4]. It should be noted that the absence of the D2 capacitance signature in the relaxed measurement reduces the overall capacitance signal,

ACCEPTED MANUSCRIPT

15 September 2024 04:34:55

AIP Publishing
This manuscript was accepted by Appl. Phys. Lett. Click here to see the version of record.

Fig. 1. Capacitance vs. frequency at various temperatures for CZTSSe under (a) relaxed conditions and (b) following a carrier injection pretreatment. Capacitance vs. temperature at various frequencies of the same CZTSSe device under (c) relaxed conditions and (d) following a carrier injection pretreatment.

even at room temperature. Relaxation at low temperature in the dark is required to recover the behavior observed for the relaxed measurement at all temperatures. Note that this behavior is reversible; following a relaxation event the CIP capacitance spectra can be recovered by performing another CIP treatment.

Assuming the capacitance response originates from a defect, the data was further analyzed to quantify the activation energies associated with the capacitance signatures following a thermally activated trap response, described by Eqn. (1)[7]:

$$\omega_0 = A_0 T^2 \exp\left[\frac{-E_A}{kT}\right] \quad (1)$$

where ω_0 is the demarcation angular frequency, A_0 is the temperature independent prefactor, and E_A is the defect activation energy. A_0T^2 represents the product of the valence band density of state (N_V, $\propto T^{3/2}$), thermal velocity of carriers ($\langle v_{th}\rangle$, $\propto T^{1/2}$), and the electron capture cross section (σ_n). Arrhenius plots of the relaxed and CIP capacitance signatures are shown in Figs. 2(a) and (b) respectively. The single capacitance signature from the relaxed measurement has an activation energy of 59 ± 3 meV, while the two observed capacitance signatures in the CIP measurement result in defect activation energies of 90 ± 2 meV (D1) and 157 ± 2 meV (D2). Additionally, the exponential prefactor A_0 increases for the sample measured under CIP conditions relative to the relaxed measurement, from c. 6×10^4 $s^{-1}K^{-2}$ to c. 1.2×10^6 $s^{-1}K^{-2}$ (D1) and 5×10^5 $s^{-1}K^{-2}$ (D2). We attribute the observed increase in A_0 to σ_n, as expected due to the increasing E_A in accordance with the Meyer-Neldel rule.[17]

Defect energetic profiles, shown in Fig. 2(c), were constructed using the method described by Walter et al.[18] where E_t (see Eq. S1 in the SI) was calculated using the A_0 values extracted from the Arrhenius fits. The ordinate of these profiles is proportional to the density of defects while the abscissa is the energy relative to the valence band. Note that the CIP profile has a transition from using $A_{0,D1}$ to $A_{0,D2}$ at 115 meV. The relaxed sample has a single lower energy peak (c. 60 meV) and what appears to be a very broad peak (c. 100-150 meV). These results demonstrate how large an impact metastable defects in CZTSSe have on AS results. Weiss et al.[5] completed this analysis using pure selenide CZTSe fabricated from co-evaporation process which showed a similar distribution as the CIP method.

Fig. 2. Arrhenius plots of Eq. 1 for the CZTSSe device (a) under relaxed conditions and (b) with the carrier-injection pretreatment. (c) Defect energetic profiles illustrating the density of defect states for the CZTSe device with a carrier-injection pretreatment (black circles) and under relaxed measurement conditions (blue crosses).

It is clear that carrier injection causes a significant change in the admittance spectroscopy measurements. This is important because AS is often combined with IV(T) measurements, or devices are exposed to light before/during measurement, which can significantly alter the AS results and extracted defect properties for kesterites. As metastable response is measured following carrier-injection (i.e. forward bias or light), we attribute this effect to charge trapping following

ACCEPTED MANUSCRIPT

15 September 2024 04:34:55

AIP Publishing

This manuscript was accepted by Appl. Phys. Lett. Click here to see the version of record.

carrier injection. Charge trapping/carrier localization has also previously been reported for kesterites from TRPL[14] and time-resolved terahertz spectroscopy[15]. Such charge trapping is especially important at low temperature as thermal emission from a trap state is exponential dependent on the temperature. The increase in activation energy of the lower energy D1 defect following the CIP is attributed to charge trapping, which can alter the local energetic potential influencing the capture cross section and/or defect potential. This has similarly been reported in $CISe_2$ where the change in the charge state of a defect results in large lattice relaxation, which consequently shifts the energetic level of the defect to lower energy.[19] Here, low temperature relaxation is required to relax the absorber as it removes trapped charges higher than thermalization and therefore ensures subsequent higher temperature measurements do not need further relaxation.

Finally, voltage-dependent admittance spectroscopy was completed in order to determine the nature of the measured capacitance signatures, analyses of which is described by Deocock et al.[20] All measurements were completed following CIP measurement conditions, as voltage-dependent measurements inherently results in carrier injection in forward bias. Linear fits to the Arrhenius plots were optimized simultaneously with the assumption that N_V, $\langle v_{th} \rangle$, and σ_n are voltage independent. Once the mean squared error was minimized on all fits, the activation energies extracted from the slopes were plotted vs. voltage shown in Fig. 3(a). We find both the D1 and D2 activation energies are independent of voltage, which is similarly reported by Sun et al.[21] Since the activation energies are voltage independent, these capacitance signatures are not likely to originate from the interface. If the response did originate from the interface, we expect the activation energy would change with voltage since the distance between the Fermi level and the conduction band at the interface also changes significantly with voltage.[22] Note that this assumes a continuous distribution of defect states at the interface, no Fermi level pinning, and the n-type layer dominates the admittance response in this region resulting in electrons as the majority carrier.

Fig. 3. (a) Activation energies of the D1 and D2 admittance signatures at different DC-voltage biases for a CZTSSe device following carrier-injection pretreatment. (b) Defect distributions of a CZTSSe device using a carrier-injection pretreatment under 0 V_{DC} and -1 V_{DC} biasing aligned using the exponential prefactor values from the Arrhenius fits and (c) the D1 and D2 peak values from the Gaussian distribution fits as a function of V_{DC}. The best fit line in (c) is $\propto (V_{BI}-V_{DC})^{-1}$.

Defect energetic profiles were also constructed from the voltage dependent AS measurements and fit with Gaussian distributions; fitting parameters are listed in Table S1. Fig. 3(b) shows the 0 V_{DC} and -1 V_{DC} case (created using the same method as Fig. 2(c)). Fig. 3(c) shows the peak values of the D1 and D2 energetic profiles as a function of DC voltage. We find the peak values of the energetic profiles are voltage-independent for D1, while D2 shows an increase in forward bias. As the peak of the energetic profiles of the D1 signature is voltage independent, we interpret this signature as being related to carrier freezeout; shallow level defects are no longer responding to the probing signal.[20] This conclusion requires the absorber layer to be almost entirely depleted (in which case the depletion capacitance is voltage-independent) resulting in the geometric capacitance for values below the D1 response.

It is obvious the D2 defect is primarily a metastable defect and is only electrically active following carrier injection. The D2 peak values (i.e. the magnitude of the fitted Gaussian

ACCEPTED MANUSCRIPT

15 September 2024 04:34:55

AIP Publishing

This manuscript was accepted by Appl. Phys. Lett. Click here to see the version of record.

distributions at $E_{A,D2}$) plotted in Fig. 3(c) are $\propto (V_{BI}-V_{DC})^{-1}$ as shown by the best fit line, where V_{BI} is the built in potential (0.48 V, estimated from the Mott-Schottky plot at 142 K). Note that this temperature was chosen for the V_{BI} estimate as the D2 capacitance signature in Fig. 1(b) is clearly defined at 142 K. Therefore, we conclude this defect has a parabolic defect spatial distribution.[20]

In conclusion, we have demonstrated the large impact metastable behavior in CZTSSe has on admittance spectroscopy measurements by comparing a device under electrically and optically relaxed conditions and with a carrier-injection pretreatment. The relaxed measurement contains a single capacitance signature while the carrier-injection pretreatment contains two capacitance signatures. Additionally, voltage dependent admittance spectroscopy demonstrates the activation energy associated with these two capacitance signatures are voltage independent and suggest an origin due to bulk defect responses. These results indicate the higher energy metastable capacitance signature is activated by charge trapping within the absorber layer. Therefore, it is recommended that great care and consideration must be taken when measuring and analyzing non-ideal and metastable devices using admittance spectroscopy as the electrical and optical history of the device can greatly impact the results and can explain the wide variations reported in admittance for kesterites.

Supplementary Material

See supplementary material for additional information including the light and dark IV response of the tested solar cell, the equivalent AC circuit model, and additional information on the Gaussian fits of the defect energetic profiles.

Acknowledgments

This work was supported by the DOE through a non-proprietary partnering (NPO) with NREL, NSF Solar Economy IGERT 0903670-DGE, and the Solar Energy Research Institute for India and the United States (SERIIUS) DE AC36-08G028308. The authors would like to thank Dr. Sukgeun Choi for his assistance and discussion throughout the NPO project.

References

1. Walsh, A., Chen, S., Wei, S.-H. & Gong, X.-G. Kesterite Thin-Film Solar Cells: Advances in Materials Modelling of Cu2ZnSnS4. *Adv. Energy Mater.* **2,** 400–409 (2012).
2. Mitzi, D. B., Gunawan, O., Todorov, T. K., Wang, K. & Guha, S. The path towards a high-performance solution-processed kesterite solar cell. *Sol. Energy Mater. Sol. Cells* **95,** 1421–1436 (2011).
3. Gunawan, O., Gokmen, T., Warren, C. W., Cohen, J. D., Todorov, T. K., Barkhouse, D. A. R., Bag, S., Tang, J., Shin, B. & Mitzi, D. B. Electronic properties of the Cu2ZnSn(Se,S)4 absorber layer in solar cells as revealed by admittance spectroscopy and related methods. *Appl. Phys. Lett.* **100,** 253905 (2012).
4. Levcenko, S., Just, J., Redinger, A., Larramona, G., Bourdais, S., Dennler, G., Jacob, A. & Unold, T. Deep Defects in Cu2ZnSn(S,Se)4 Solar Cells with Varying Se Content. *Phys. Rev. Appl.* **5,** 24004 (2016).
5. Weiss, T. P., Redinger, A., Regesch, D., Mousel, M. & Siebentritt, S. Direct Evaluation of Defect Distributions From Admittance Spectroscopy. *IEEE J. Photovoltaics* **4,** 1665–1670

ACCEPTED MANUSCRIPT

15 September 2024 04:34:55

AIP Publishing

This manuscript was accepted by Appl. Phys. Lett. Click here to see the version of record.

(2014).
6. Li, J. V., Kuciauskas, D., Young, M. R. & Repins, I. L. Effects of sodium incorporation in Co-evaporated Cu2ZnSnSe4 thin-film solar cells. *Appl. Phys. Lett.* **102,** 163905 (2013).
7. Heath, J. & Zabierowski, P. in *Adv. Charact. Tech. Thin Film Sol. Cells* (eds. Abou-Ras, D., Kirchartz, T. & Rau, U.) 93–119 (Wiley-VCH Verlag GmbH & Co. KGaA, 2016). doi:10.1002/9783527699025.ch4
8. Hages, C. J., Carter, N. J., Moore, J., McLeod, S. M., Miskin, C. K., Lundstrom, M. S., Agrawal, R., Joglekar, C., Lundstrom, M. S. & Agrawal, R. Device comparison of champion nanocrystal-ink based CZTSSe and CIGSSe solar cells: Capacitance spectroscopy. in *Photovolt. Spec. Conf. (PVSC), 2013 IEEE 39th* 1966–1971 (Ieee, 2013). doi:10.1109/PVSC.2013.6744856
9. Eisenbarth, T., Caballero, R., Nichterwitz, M., Kaufmann, C. A., Schock, H.-W. & Unold, T. Characterization of metastabilities in Cu(In,Ga)Se2 thin-film solar cells by capacitance and current-voltage spectroscopy. *J. Appl. Phys.* **110,** 94506 (2011).
10. Heath, J. T., Cohen, J. D. & Shafarman, W. N. Bulk and metastable defects in CuIn1−xGaxSe2 thin films using drive-level capacitance profiling. *J. Appl. Phys.* **95,** 1000–1010 (2004).
11. Hages, C. J., Moore, J., Dongaonkar, S., Alam, M., Lundstrom, M. & Agrawal, R. Device limitations and light-soaking effects in CZTSSe and CZTGeSSe. in *2012 38th IEEE Photovolt. Spec. Conf.* 002658–002663 (IEEE, 2012). doi:10.1109/PVSC.2012.6318142
12. Grenet, L., Grondin, P., Coumert, K., Karst, N., Emieux, F., Roux, F., Fillon, R., Altamura, G., Fournier, H., Faucherand, P. & Perraud, S. Experimental evidence of light soaking effect in Cd-free Cu2ZnSn(S,Se)4-based solar cells. *Thin Solid Films* **564,** 375–378 (2014).
13. Hages, C. J., Carter, N. J. & Agrawal, R. Generalized quantum efficiency analysis for non-ideal solar cells: Case of Cu2ZnSnSe4. *J. Appl. Phys.* **119,** 14505 (2016).
14. Hages, C. J., Redinger, A., Levcenko, S., Hempel, H., Koeper, M. J., Agrawal, R., Greiner, D., Kaufmann, C. A. & Unold, T. Identifying the Real Minority Carrier Lifetime in Nonideal Semiconductors: A Case Study of Kesterite Materials. *Adv. Energy Mater.* **1700167,** 1700167 (2017).
15. Hempel, H., Redinger, A., Repins, I., Moisan, C., Larramona, G., Dennler, G., Handwerg, M., Fischer, S. F., Eichberger, R. & Unold, T. Intragrain charge transport in kesterite thin films—Limits arising from carrier localization. *J. Appl. Phys.* **120,** 175302 (2016).
16. Miskin, C. K., Yang, W.-C., Hages, C. J., Carter, N. J., Joglekar, C. S., Stach, E. A. & Agrawal, R. 9.0% efficient Cu 2 ZnSn(S,Se) 4 solar cells from selenized nanoparticle inks. *Prog. Photovoltaics Res. Appl.* **23,** 654–659 (2015).
17. Herberholz, R., Walter, T., Müller, C., Friedlmeier, T., Schock, H. W., Saad, M., Lux-Steiner, M. C. & Alberts, V. Meyer–Neldel behavior of deep level parameters in heterojunctions to Cu(In,Ga)(S,Se)2. *Appl. Phys. Lett.* **69,** 2888 (1996).
18. Walter, T., Herberholz, R., Müller, C. & Schock, H. W. Determination of defect distributions from admittance measurements and application to Cu(In,Ga)Se2 based heterojunctions. *J. Appl. Phys.* **80,** 4411–4420 (1996).
19. Igalson, M. & Schock, H. W. The metastable changes of the trap spectra of CuInSe2-based photovoltaic devices. *J. Appl. Phys.* **80,** 5765–5769 (1996).
20. Decock, K., Khelifi, S., Buecheler, S., Pianezzi, F., Tiwari, A. N. & Burgelman, M. Defect distributions in thin film solar cells deduced from admittance measurements under

ACCEPTED MANUSCRIPT

15 September 2024 04:34:55

AIP Publishing

This manuscript was accepted by Appl. Phys. Lett. Click here to see the version of record.

different bias voltages. *J. Appl. Phys.* **110,** 63722 (2011).

21. Sun, X., Hages, C. J., Carter, N. J., Moore, J. E., Agrawal, R. & Lundstrom, M. Characterization of nanocrystal-ink based CZTSSe and CIGSSe solar cells using voltage-dependent admittance spectroscopy. in *2014 IEEE 40th Photovolt. Spec. Conf.* **2,** 2416–2418 (IEEE, 2014).
22. Nicollian, E. H. & Goetzberger, A. MOS CONDUCTANCE TECHNIQUE FOR MEASURING SURFACE STATE PARAMETERS. *Appl. Phys. Lett.* **7,** 216–219 (1965).

ACCEPTED MANUSCRIPT

15 September 2024 04:34:55

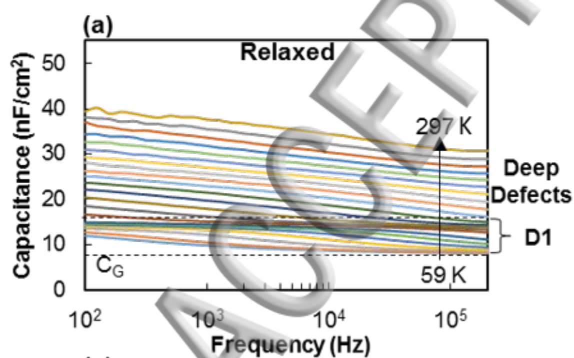

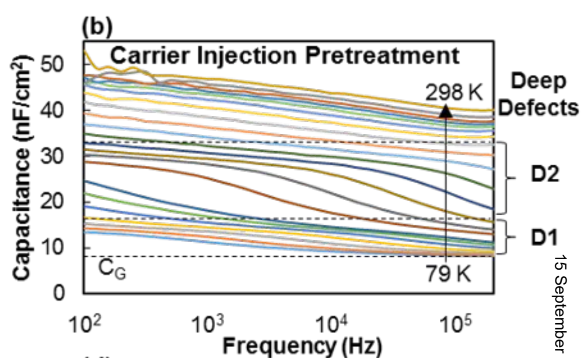

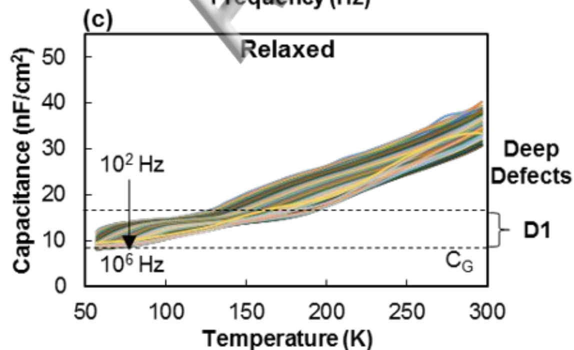

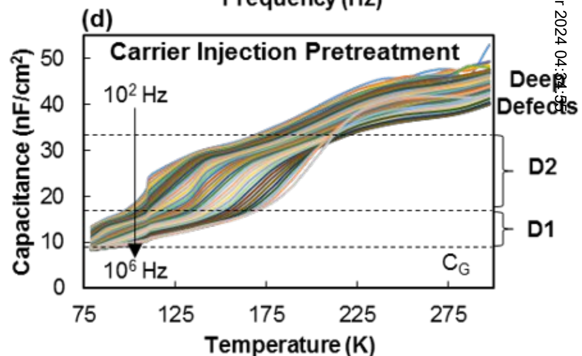

ACCEPTED
15 September 2024 04:34:55

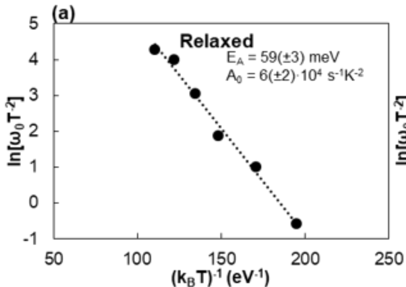

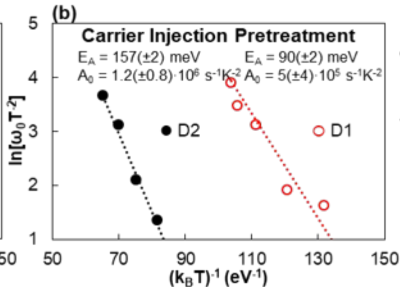

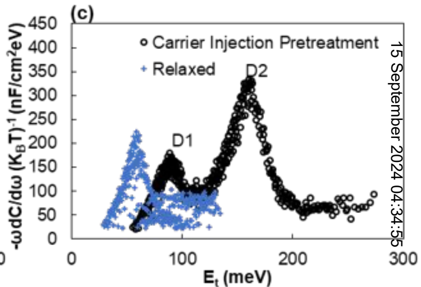

15 September 2024 04:34:55

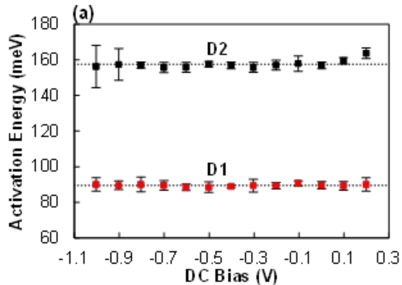

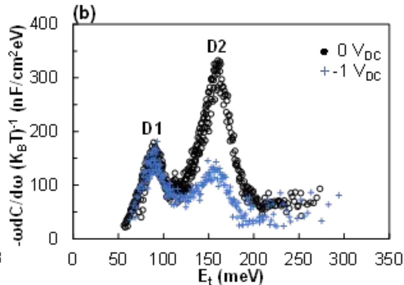

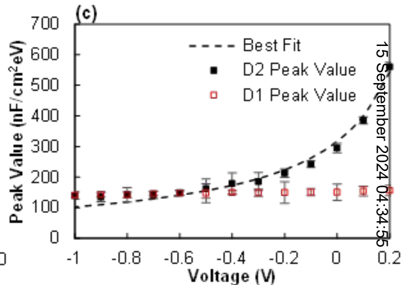

15 September 2024 04:34:55